J|A|C|S
ARTICLES
Published on Web 12/20/2001

An NMR Investigation of CO Tolerance in a Pt/Ru Fuel Cell Catalyst

YuYe Tong, Hee Soo Kim, Panakkattu K. Babu, Piotr Waszczuk, Andrzej Wieckowski,* and Eric Oldfield*

Contribution from the Department of Chemistry, University of Illinois at Urbana-Champaign, 600 South Mathews Avenue, Urbana, Illinois 61801

Received July 16, 2001

Abstract: We report the first combined application of solid-state electrochemical NMR (EC NMR), cyclic voltammetry (CV), and potentiostatic current generation to investigate the topic of the ruthenium promotion of MeOH electro-oxidation over nanoscale platinum catalysts. The CV and EC NMR results give evidence for two types of CO: CO on essentially pure Pt and CO on Pt/Ru islands. There is no NMR evidence for rapid exchange between the two CO populations. CO molecules on the primarily Pt domains behave much like CO on pure Pt, with there being little effect of Ru on the Knight shift or on Korringa relaxation. In sharp contrast, COs on Pt/Ru have highly shifted ^{13}C NMR resonances, much weaker Korringa relaxation, and, at higher temperatures, they undergo thermally activated surface diffusion. For CO on Pt, the correlation observed between the $2\pi^*$ Fermi level local density of states and the steady-state current suggests a role for Ru in weakening the Pt−CO bond, thereby increasing the CO oxidation rate (current). The combined EC NMR/electrochemistry approach thus provides new insights into the promotion of CO tolerance in Pt/Ru fuel cell catalysts, in addition to providing a novel route to investigating promotion in heterogeneous catalysis in general.

Introduction

Fuel cells are much more efficient than conventional power generation sources, may use unconventional fuels, and can also operate without atmospheric contamination.[1] However, since many fuel cell reactions occur at relatively low temperatures, catalyst poisoning is often a problem, and typical platinum catalysts must be combined with other transition metals to display satisfactory behavior.[2,3] The nature of such catalyst promotion is, however, poorly understood. In our group, we have been interested in investigating the direct methanol oxidation fuel cell (DMFC) for some time. The DMFC runs on methanol, and CO is an intermediate in MeOH oxidation:

$$Pt + CH_3OH \rightarrow Pt{-}CO + 4H^+ + 4e^- \quad (1)$$

CO chemisorption significantly degrades fuel cell performance, and since CO is always present, an effective means for increasing the CO tolerance of these (and other) fuel cell catalysts is necessary.[4] Fortunately, it has been found that the addition of ruthenium to Pt catalysts is highly beneficial, since ruthenium promotes CO oxidation (to CO_2) via the so-called bifunctional mechanism:[3]

$$Pt{-}CO + Ru{-}OH \xrightarrow{k} Pt + Ru + CO_2 + H^+ + e^- \quad (2)$$

where OH symbolizes an oxygen-containing species, and k is the reaction rate constant. The exact details of the electronic and dynamic aspects of this mechanism, though, are not well understood. Here, we show that electrochemical nuclear magnetic resonance spectroscopy (EC NMR)[5−8] may help provide new insights into the Ru promotion process by probing in a direct way the electronic structure of the Pt/Ru catalyst surface. The EC NMR technique gives important information on the diffusional behavior of CO on such bimetallic catalysts as well as an interesting relationship between electrochemical current generation and the Fermi level local density of states (E_f-LDOS) of CO on Pt.

Experimental Section

Sample Preparation and Electrochemistry. Pt/Ru nanoparticle catalysts were prepared using commercial fuel cell grade platinum black (Johnson-Matthey, micrometer-sized agglomerates comprised of ca. 10 nm Pt nanoparticles) as substrates for the spontaneous deposition of ruthenium from an aqueous solution of $RuCl_3$.[9] Samples were prepared

(1) Special Issue on Energy. *Science* **1999**, *285*, 682−685.
(2) Reddington, E.; Sapienza, A.; Gurau, B.; Smotkin, E. S.; Mallouk, T. E. *Science* **1998**, *280*, 1735−1737.
(3) Hamnett, A. In *Interfacial Electrochemistry: Theory, Experiment, and Applications*; Wieckowski, A., Ed.; Marcel Dekker: New York, 1999; pp 843−883.
(4) Carrette, L.; Friedrich, K. A. *ChemPhysChem* **2000**, *1*, 162−193. Pettersson, L. J.; Westerholm, R. *Int. J. Hydrogen Energy* **2001**, *26*, 243−264.
(5) Slezak, P. J.; Wieckowski, A. *J. Magn. Reson., Ser. A* **1993**, *102*, 166−172.
(6) Yahnke, M. S.; Rush, B. M.; Reimer, J. A.; Cairns, E. J. *J. Am. Chem. Soc.* **1996**, *118*, 12250−12251.
(7) Wu, J.; Day, J. B.; Franaszczuk, K.; Montez, B.; Oldfield, E.; Wieckowski, A.; Vuissoz, P.-A.; Ansermet, J.-Ph. *J. Chem. Soc., Faraday Trans.* **1997**, *93*, 1017−1026.
(8) Rush, B. M.; Reimer, J. A.; Cairns, E. J. *J. Electrochem. Soc.* **2001**, *148*, A137−A148.
(9) Waszczuk, P.; Solla-Gullón, J.; Kim, H.-S.; Tong, Y. Y.; Aldaz, A.; Wieckowski, A. *J. Catal.* **2001**, *203*, 1−6.

10.1021/ja011729q CCC: $22.00

in parallel for both NMR and electrochemical experiments. The packing density of ruthenium (the ratio of the number of Ru atoms to the number of Pt surface atoms) was estimated by inductively coupled plasma spectroscopy and cyclic voltammetry.[9] Spontaneous deposition creates ruthenium islands on the Pt support which have essentially monatomic thickness.[10] Four Pt/Ru samples, having packing densities of 0, 0.14, 0.35, and 0.52, were studied and will be referred to as Pt/Ru-0 (i.e., pure Pt), Pt/Ru-14, Pt/Ru-35, and Pt/Ru-52, respectively.

For electrochemical measurements, the supporting electrolyte was 0.5 M H_2SO_4. All potentials were referred to a hydrogen electrode reference, RHE. The oxidation current stabilized at 10 h and was taken to be the steady-state condition.

Methanol was chemisorbed as surface CO onto all Pt/Ru samples at 0.19 V. After 12 h of methanol adsorption, excess methanol was removed by rinsing with 0.5 M H_2SO_4, and the amount of CO adsorbed was monitored by cyclic voltammetry (CV) using a slow scan rate. After such prolonged adsorption, the total CO coverage on the surface, as obtained from CO stripping voltammetry, was ca. 0.9 indicating that CO is adsorbed not only on platinum but also on ruthenium.

NMR Spectroscopy. ^{13}C NMR spectra were obtained on 8.47 and 14.1 T "home-built" NMR spectrometers, which consist of 8.47 and 14.1 T $3^1/_2$ in. bore superconducting solenoid magnets (Oxford Instruments, Osney Mead, Oxford, U.K.), Tecmag (Houston, Texas) Aries pulse programmers, and a variety of other digital and radio frequency circuitries, basically as described previously.[11] To obtain samples for NMR measurements, ca. 500 mg of catalyst was used, with ^{13}C (99%) enriched methanol being introduced into the cell at 0.19 V. After 12 h of adsorption, excess methanol was removed by rinsing with 0.5 M D_2SO_4 electrolyte, and the catalysts were transferred into precleaned NMR ampules, together with a small portion of electrolyte, and were then flame-sealed. Small portions of the catalyst samples were left in the cell for electrochemical measurements. The NMR samples were studied in a home-built solenoidal NMR probe, housed in an Oxford Instruments CF-1200 cryostat.

Results and Discussion

Voltammetric Aspects. We show in Figure 1 the potentiostatic currents generated in methanol electro-oxidation at 0.3 V versus RHE as a function of time for Pt/Ru-0 (black), Pt/Ru-14 (red), Pt/Ru-35 (blue), and Pt/Ru-53 (green) catalysts. The highest steady-state currents (at ~10 h) are found with the Pt/Ru-35 and Pt/Ru-53 samples and represent a factor of 20 enhancement in activity versus the pure Pt electrode sample, Figure 1. We then investigated these same samples by using cyclic voltammetry (CV). As shown in Figure 2, there are clearly two main features: a "Pt/Ru-0" feature at ~0.53 V (black CV trace in Figure 2) which moves to a more negative potential as the amount of Ru increases, together with the appearance of a new peak at a more negative potential, on Ru addition. This is the first observation of two CO stripping peaks on a nanoscale bimetallic Pt/Ru electrode, but it is consistent with the observations of two stripping peaks on single-crystal Pt(111)/Ru reported recently.[12] Apparently, the conditions required for such observations are (i) a (heterogeneous) Ru-island-covered Pt surface and (ii) a high surface packing of CO.

The total CO coverage on the four surfaces is also constant in all four of our samples, ca. 0.9. On the basis of the results of

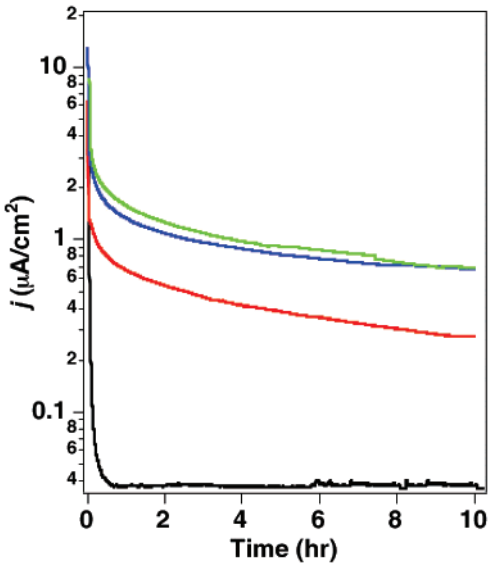

Figure 1. Electrochemical potentiostatic currents at 0.3 V vs RHE for, respectively, Pt/Ru-0 (black), Pt/Ru-14 (red), -35 (blue), and -53 (green). The highest steady-state currents at 10 h represent an ca. 20-fold enhancement in activity as compared to that of the pure Pt electrode.

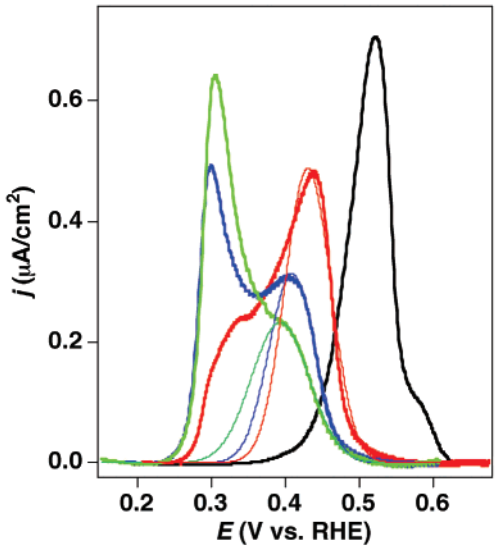

Figure 2. Electrochemical CO stripping voltammograms (at 10 mV/min) after 12 h of methanol adsorption at 0.19 V vs RHE for, respectively, Pt/Ru-0 (black), Pt/Ru-14 (red), -35 (blue), and -53 (green). These results demonstrate a new, low-potential peak which grows in as the Ru packing density increases. The thin lines represent Gaussian fits to the high-potential peak. See the text for a more detailed analysis.

experiments made on separate Pt and Pt/Ru alloy electrodes[13] and from computer simulations,[14] it is known that CO oxidizes at less positive potentials on Pt/Ru than it does on a clean Pt surface. Thus, the separation between the two voltammetric stripping maxima most likely indicates that some CO molecules are chemisorbed onto the "pure" Pt phase of the Pt/Ru electrode (the oxidation peak at high potential) while the others are on or next to Pt/Ru domains (the low potential peaks). By assuming that the high-potential peak can be represented by a Gaussian (the thinner lines in Figure 2), as suggested by the stripping

(10) Crown, A.; Moraes, I. R.; Wieckowski, A. *J. Electroanal. Chem.* **2001**, *500*, 333−343.
(11) Tong, Y. Y.; Rice, C.; Wieckowski, A.; Oldfield, E. *J. Am. Chem. Soc.* **2000**, *122*, 1123−1129.
(12) Massong, H.; Wang, H. S.; Samjeske, G.; Baltruschat, H. *Electrochim. Acta* **2000**, *46*, 701−707.
(13) Gasteiger, H. A.; Markovic, N.; Ross, P. N., Jr.; Cairns, E. J. *J. Phys. Chem.* **1994**, *98*, 617−625.
(14) Koper, M. T. M.; Lukkien, J. J.; A, P. J. J.; van Santen, R. A. *J. Phys. Chem. B* **1999**, *103*, 5522−5529.

peak of the Pt/Ru-0 electrode shown in Figure 2, these results indicate that the distribution of the charge density (i.e., the CO distribution) between the high- and low-potential peaks for the Pt/Ru-14, -35, and -52 catalyst samples is 0.66/0.34, 0.45/0.55, and 0.38/0.62, respectively, after normalization to the total oxidation charge. That is, progressively more COs are oxidized at low potential as the Ru packing density increases. This proposal is strongly supported by the quantitative NMR results, described below in detail.

While the experimental observation of such a peak separation in the stripping voltammogram is new, such an effect was in fact predicted theoretically. Specifically, by using a lattice gas model for CO electro-oxidation and dynamic Monte Carlo simulations, Koper et al.[14] investigated the role of CO mobility on CO electro-oxidation processes over a broad range of Pt/Ru compositions. On their island-covered heterogeneous surfaces, as in our samples, two CO stripping peak maxima were predicted. A peak at low potential was assigned to CO oxidation on Pt sites next to the ruthenium island edge, while a high potential peak was attributed to CO oxidation on Pt atoms much further away from the Ru sites.[13,14] Our experimental CV results support these theoretical predictions, although the theoretical model assumes virtually no surface diffusion to generate the well-resolved peak separations, while our previous NMR studies have suggested that surface diffusion does in fact occur.[15] No electronic modifications were considered in the theoretical model, and the diffusion coefficient, if different from zero, was assumed to be constant over the entire surface. These differences between the theoretical model and our results can, however, be clarified by the use of EC NMR.

The electrochemical model we propose, based on the data presented above, is as follows. There are two CO domains, as postulated before.[13,14] The low-potential CO stripping peak maximum is attributed to oxidation of CO on Pt sites around the periphery of the Ru islands and on the Ru islands themselves, that is, essentially Pt/Ru sites, while the high-potential peak is attributed to CO oxidation on Pt sites farther away from the Ru islands, that is, Pt sites. Diffusion between the two domains is slow, enabling the observation of the two CO stripping peaks shown in Figure 2. However, since the CO stripping peak from the platinum phase (on the right, Figure 2) is also shifted toward lower potential as the amount of ruthenium on the surface increases, it seems possible that the Pt phase of the surface may undergo at least some long-range modifications in its electronic structure, due to the presence of ruthenium. If this model is correct, then we would expect to find major differences in the NMR shifts and relaxation behavior of CO in the two domains, and it should also be possible to make a quantitative analysis of their Fermi level local densities of state. While there is in fact no need for such an E_f-LDOS change for the CO/Pt peak, it does, in fact, occur, as discussed below.

Electrochemical NMR. The NMR observables of interest are the Knight shift, K, and the Korringa product, T_1T, where T_1 is the nuclear spin−lattice relaxation time, and T is the temperature at which T_1 is measured. Both observables are determined by the finite and quasi-continuous nature of the Fermi level local density of states (E_f-LDOS) and represent the two major NMR probes of electronic structure in metals, in general, and of surface molecular bonding, in particular.[16] By measuring the total ^{13}C shift, from which K is extracted, and the nuclear spin−lattice relaxation time T_1, from which T_1T is obtained, the value of the E_f-LDOS can be deduced.[11] In addition, the simple but unique Korringa relationship, T_1T is a constant, enables the ready detection of the presence of other relaxation mechanism(s), for example, surface diffusion. NMR can also be used to determine whether diffusion between two different groups of nuclei is fast (on the NMR time scale of hundreds of microseconds) since rapid diffusion enables nuclei from different groups to establish a common relaxation behavior. Otherwise, they behave differently. As such, EC NMR is a very valuable complement to more classical electrochemical methods since it directly provides electronic structure information.

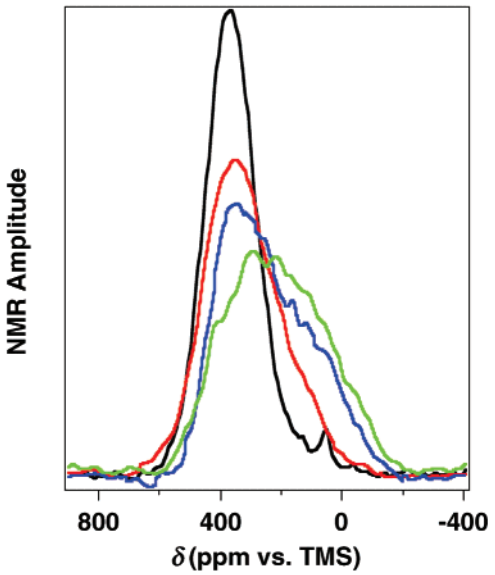

Figure 3. Spin−echo mapped ^{13}C NMR spectra of chemisorbed CO taken at room temperature for, respectively, Pt/Ru-0 (black), Pt/Ru-14 (red), -35 (blue), and -53 (green). A new high-field feature grows in as the Ru packing density increases.

We show in Figure 3 ^{13}C EC NMR results for the four Pt/Ru catalyst samples whose CV behaviors were presented in Figure 2. A new, high-field NMR feature (at lower ppm values, on the right) appears as the Ru content increases (same color code as Figures 1 and 2), and the intensity of this feature also increases with Ru level. Such a high-field feature has not been reported previously in any NMR studies of CO chemisorption, either by (dry sample) surface NMR or by EC NMR. Since the results of Figure 2 suggest two CO domains (by CV), the ^{13}C NMR spectra of all four samples shown in Figure 3 were therefore simulated by using two Gaussians, Table 1 and insets in Figure 4B−D. The fractions of the COs on Pt/Ru sites obtained from the ^{13}C NMR spectral deconvolutions were 0.23, 0.54, and 0.63 for Pt/Ru-14, -35, and -52, respectively. Moreover, as shown in Figure 5, these quantitative population results track almost exactly those obtained from the CO stripping voltammograms (Figure 2). In particular, the correlation shown in Figure 5 has a slope of 1.0, an R^2 value of 0.94, and an essentially zero intercept. These results clearly support the two-

(15) Day, J. B.; Vuissoz, P.-A.; Oldfield, E.; Wieckowski, A.; Ansermet, J.-P. *J. Am. Chem. Soc.* **1996**, *118*, 13046−13050.

(16) van der Klink, J. J.; Brom, H. B. *Prog. Nucl. Magn. Reson. Spectrosc.* **2000**, *36*, 86−201.

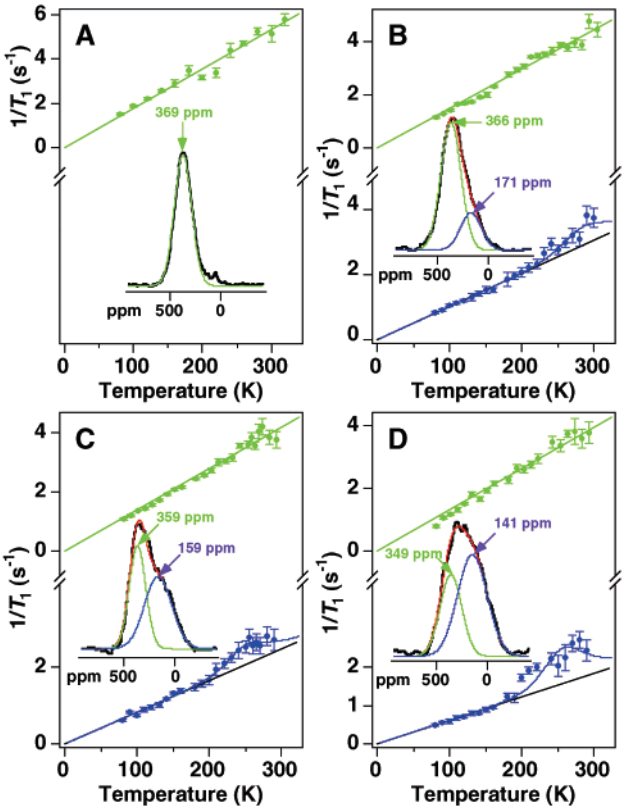

Figure 4. Temperature dependencies of the ^{13}C NMR nuclear spin−lattice relaxation rates for ^{13}CO on A, Pt; B, Pt/Ru-14; C, Pt/Ru-35; and D, Pt/Ru-53. The insets show the corresponding spectra and double-Gaussian deconvolutions with color-matching arrows indicating the spectral positions (green for high- and blue for low-frequency Gaussian peaks with red for the sum) at which the relaxation rates were measured. The straight lines are the Korringa fits (to data taken at the 10 lowest T points in B−D for the low-frequency Gaussian peak), showing that chemisorbed CO at the metal surface acquires metallic properties. The values of the Korringa constant, T_1T, at these peak positions are shown in Table 1. The deviations from pure Korringa behavior at high temperature in B−C indicate the onset of a thermally activated CO diffusion process. The solid curves are the fits to eq 3, from which the diffusion activation energies were obtained.

Table 1. Double-Gaussian Deconvolution of ^{13}C NMR Spectra and the Corresponding T_1 Data

		Pt/Ru-0	Pt/Ru-14	Pt/Ru-35	Pt/Ru-52
	fraction	0	0.23	0.54	0.63
low freq	peak (ppm)		171	159	141
	T_1T (s K)		98.2	120.0	160.7
	fraction	1.00	0.77	0.46	0.37
high freq	peak (ppm)	369	366	359	349
	T_1T (s K)	59.3	66.9	71.1	75.2

domain model proposed from the electrochemical measurements, as well as from the theoretical modeling results.[14]

The position of the low-field peak changes by only 20 ppm as a function of Ru content, from 369 ppm for Pt/Ru-0 to 366, 359, and 349 ppm for Pt/Ru-14, -35, and -52, respectively (Figure 4). In addition, changes in the corresponding Korringa constants, T_1T, are relatively small (Table 1). These observations indicate that CO molecules resonating at low-field, assigned to COs on Pt sites away from Ru islands, experience relatively weak electronic perturbations caused by Ru deposition. In sharp contrast, CO molecules resonating at high-field, assigned to COs on Pt/Ru sites (Ru islands and their peripheries), experience much stronger electronic perturbations. The high-field peak position changes from 369 ppm for Pt/Ru-0 to 171, 159, and

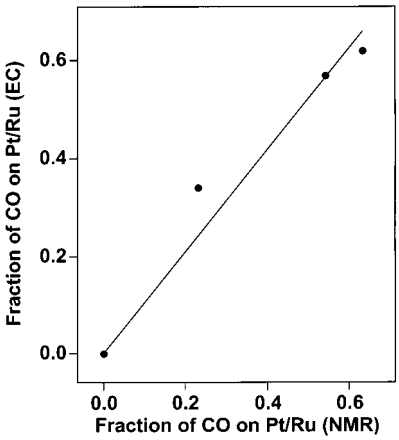

Figure 5. Correlation between the fractions of CO on Pt/Ru sites obtained by electrochemical CO stripping, Figure 2, and by ^{13}C NMR, Figure 3. The straight line represents a linear fit to the data, giving a slope of 1.0 and an R^2 of 0.94.

141 ppm for Pt/Ru-14, -35, and -52, respectively, and is accompanied by a factor of 2 increase in T_1T (Table 1). These high-field peak positions are quite different from the value of 210 ppm, the ^{13}C peak position for CO chemisorbed on pure Ru,[17] indicating that the electronic properties of the deposited Ru are strongly modified by the Pt substrate.

More specific electronic and dynamic structural information about the nature of metal−ligand interactions in these two domains was then obtained by using temperature-dependent nuclear spin−lattice relaxation measurements (T_1), and we show in Figure 4 the temperature-dependent spin−lattice relaxation rate (T_1^{-1}) results for CO on pure Pt and for the three Pt/Ru catalyst samples, measured at the spectral positions indicated. In the case of pure Pt, Figure 4A, there is no deviation from a purely Korringa relationship, that is, the data can be fitted to a straight line passing through the origin, a result which is independent of where the T_1 measurement is made. In sharp contrast, as shown in Figure 4B−D, Ru deposition causes a marked deviation in Korringa behavior, with the effect being largest at high temperatures, at high field (blue lines, on the right of the spectra), and at high Ru levels. The purely Korringa behavior still holds for T_1 measured at the high-frequency (low-field) peak on the left of the spectra. However, the relatively small changes in the Korringa constant (T_1T) and in peak position, Table 1, indicate only a weak (long-range) electronic effect caused by Ru deposition. The straight lines for T_1 measured at the low-frequency (high-field) peak positions (blue solid circles) in Figure 4B−D are the Korringa fits to data taken at the 10 lowest temperatures (<200 K). In contrast to the results for COs on Pt sites far away from Ru, these T_1T values increase significantly upon Ru decoration, indicating a strong alteration in local electronic structure. Since the Korringa relationship is a unique NMR fingerprint of the metallic state, we can conclude that all chemisorbed CO acquires metallic character after adsorption. However, of much more interest is the observation of the very major deviations from the simple Korringa relationship seen at higher temperatures for the COs on the Ru (and peripheral Pt) domains. These deviations clearly indicate the onset of a second relaxation mechanism. The solid curves in Figure 4B−D are the fits to eq 3, which take into account this

(17) Wang, P.-K.; Ansermet, J.-P.; Rudaz, S. L.; Wang, Z. Y.; Shore, S.; Slichter, C. P.; Sinfelt, J. H. *Science* **1986**, *234*, 35−41.

thermally activated process, presumably surface diffusion:

$$T_1^{-1} = aT + 2(\Delta\omega)^2\tau/(1 + \omega_0^2\tau^2) \quad (3)$$

The first term is the standard Korringa contribution in which T is the absolute temperature and a^{-1} is the Korringa constant, obtained from the straight-line fit at $T < 200$K. The second term accounts for surface diffusion, in which $\Delta\omega$ is the average local field inhomogeneity seen by a moving CO, ω_0 is the NMR Larmor frequency, and t is the correlation time. The correlation time is related to the activation energy for diffusion (E_{diff}) through the Arrhenius relation $\tau = \tau_0 \exp(E_{diff}/RT)$, where τ_0 is the preexponential factor, taken to be 10^{-13} s. The fit gives two parameters: the local field inhomogeneity ($\Delta\omega$) and the activation energy for diffusion (E_{diff}). The values obtained for $\Delta\omega/2\pi$ and E_{diff} are 3.3, 2.7, and 3.6 kHz and 5.7, 4.9, and 5.1 kcal/mol, for Pt/Ru-14, Pt/Ru-35, and Pt/Ru-52, respectively. For comparison, the activation energy for CO diffusion on pure Pt under the same electrochemical conditions has been previously determined to be 7.8 kcal/mol.[18] Clearly, the presence of Ru substantially enhances surface diffusion for the CO molecules on Pt/Ru sites, but for the Pt sites, the effects are very small.

Electronic and Dynamic Effects of Ru at Pt Surfaces. Without resorting to any detailed theoretical model, the mere fact that CO molecules resonating at high frequencies (on the left of the NMR spectra) obey the Korringa relationship over the entire experimental temperature range while those resonating at low frequencies (on the right) show a diffusional contribution at higher temperatures indicates that at least two different populations of chemisorbed CO must exist on these electrode surfaces. In one subset, diffusion is faster than in the other, and exchange (diffusion) between these two populations must be slow on the NMR time scale. These observations provide an unambiguous mechanistic interpretation of the electrochemical observation of two peaks in the CO stripping voltammograms. Specifically, there are two major populations of CO: COs located on or near Ru and undergoing fast, thermally activated diffusion (NMR and electrochemical relative intensities increasing with Ru loading) and the COs on Pt sites further away from Ru, undergoing slower diffusion (NMR and electrochemical relative intensities decreasing with Ru loading).

In terms of understanding the fundamental origins of the enhancements in CO diffusion on Pt/Ru sites, EC NMR can again provide potentially important information, this time by investigating the Fermi level local densities of states (E_f-LDOS) of both the ligand and the metal catalyst. In particular, the monotonic decrease in shift and the simultaneous increase in T_1T values as a function of Ru content, Table 1, clearly indicate the occurrence of electronic structural alterations caused by Ru, in *both* domains. By using the peak position and the corresponding T_1T values, we can estimate the E_f-LDOS at Pt sites distant from Ru of the "clean" metal surfaces (before chemisorption) by using the linear ^{13}C NMR shift versus metal surface E_f-LDOS correlation used previously[19] to deduce the 5σ- and 2π*-E_f-LDOS at ^{13}C after chemisorption.[11] These results are shown in Figure 6 (solid symbols). For COs on Pt/Ru sites, the above analysis cannot be applied directly, because the orbital contribution needed to be used as a reference for extracting the pure Knight shift is not known. However, we can make very good estimates of this simply by taking the extreme cases of purely 5σ or 2π* contributions to the NMR observables. In this way, either the 5σ or the 2π* E_f-LDOS can be deduced by using the Korringa relationship. With these E_f-LDOS values, the pure Knight shifts due to 5σ or 2π* E_f-LDOS can be readily calculated as described before, and we obtain 507, 501, and 494 ppm for 5σ and 79, 69, and 57 ppm for 2π*, respectively, for Pt/Ru-14, -35, and -52. Clearly, a purely 5σ contribution leads to unphysical results and can be discarded. However, if the purely 2π* contribution is a good approximation to the actual situation, then the orbital contribution obtained by subtracting the pure Knight shift from the experimental shift should be a constant. Using this approach, we find values of 92, 90, and 84 ppm for Pt/Ru-14, -35, and -52, giving an average value of 89 $\pm$ 3 ppm. In addition, by using 89 ppm as the orbital reference and assuming the same slope of the shift versus metal surface E_f-LDOS correlation as found for pure Pt and Pd,[19] the metal E_f-LDOS at the Pt/Ru sites can be estimated. The results thus obtained are shown in Figure 6 (open symbols) and clearly show major decreases in both metal and CO E_f-LDOS on increasing Ru coverage.

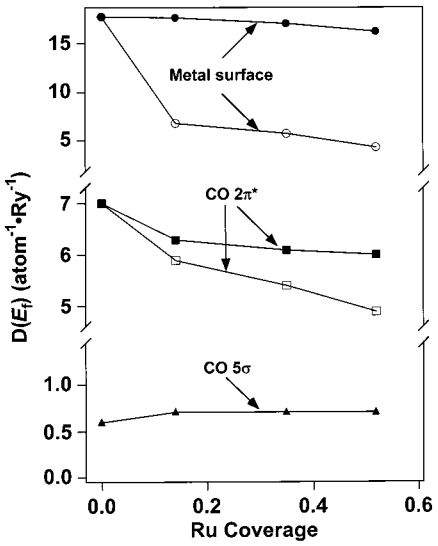

Figure 6. The metal surface E_f-LDOS before chemisorption and the 5σ and 2π* E_f-LDOS at ^{13}C after chemisorption for (remote) Pt (solid symbols) and Pt/Ru (open symbols) sites, as a function of Ru coverage.

The changes in the E_f-LDOS at Pt sites of "clean" metal surfaces, that is, away from Ru islands, as well as the 2π*-E_f-LDOS at ^{13}C, are both relatively small on increasing Ru coverage (filled symbols in Figure 6); at most they are ca. 9% for the metal surface and ca. 14% for 2π* E_f-LDOS. In sharp contrast, the E_f-LDOS values at the Pt/Ru sites (open symbols in Figure 6) greatly decrease with respect to pure Pt: an ca. 75% decrease for the metal surface and an ca. 30% decrease for the 2π* E_f-LDOS (and any possible 5σ contribution would further reduce the 2π* E_f-LDOS), reflecting very strong local electronic perturbations. This conclusion of a reduction in the metal surface E_f-LDOS can also be deduced from the results of recent in situ X-ray absorption spectroscopic studies

(18) Tong, Y. Y.; Oldfield, E.; Wieckowski, A. *Anal. Chem.* **1998**, *70*, 518A−527A.
(19) Tong, Y. Y.; Rice, C.; Godbout, N.; Wieckowski, A.; Oldfield, E. *J. Am. Chem. Soc.* **1999**, *121*, 2996−3003.

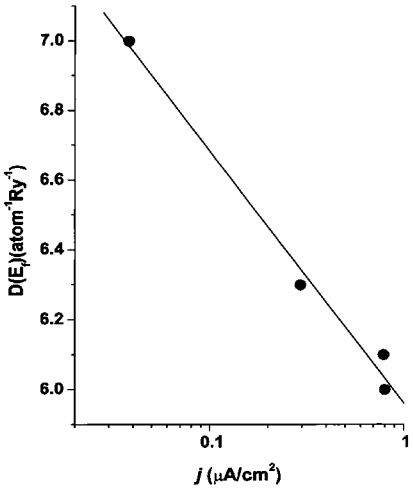

Figure 7. Graph showing correlation between the long-term (10 h) steady-state current and the $2\pi^*$ E_f-LDOS for CO on Pt sites at the catalyst surfaces. The R value of the correlation is 0.994. The p-value of the correlation is $p = 0.006$. Only the CO/Pt D(E_f) results are shown since under current generating conditions the level of CO on Pt/Ru sites is expected to be very small.

of Pt/Ru alloy nanoparticles.[20] There, it was shown that alloying Ru reduces the Pt−Pt distance. A reduction in Pt−Pt distance increases the *d*-orbital overlap between adjacent Pt atoms, thereby widening the Pt *d*-bandwidth. Consequently, the metal E_f-LDOS would be expected to decrease, as found here. And as demonstrated previously,[11,19] a decrease in the clean surface metal E_f-LDOS reduces $2\pi^*$ back-donation, thereby weakening the CO−metal bond.[21]

The EC NMR results discussed above quite clearly show a number of remarkable changes in the ^{13}C NMR spectra of CO chemisorbed to Pt−Ru electrodes. Moreover, there is an excellent correlation between the NMR and electrochemical results in terms of the relative areas or assignments of CO to Pt or Pt/Ru "domains". Since it is also known that the actual catalytic *activity* of the different catalyst samples is very different (Figure 1), it appeared to us to be worth investigating if there was any correlation between the NMR and catalytic activity results, since they might form the basis for future detailed investigations of, for example, promotion effects using electronic and, potentially, diffusion information. While the very complex nature of the methanol oxidation process is certainly a given, it is, nevertheless, interesting to see if such correlations do in fact exist.

Figure 7 shows the correlation observed between the CO's $2\pi^*$ E_f-LDOS and the steady-state current (from Figures 1 and 6). For CO on the Pt-rich domains, we find a linear correlation between D(E_f) and ln j having an R value of 0.994 and a p value of 0.006. Clearly then, the current increases exponentially with a decrease in back-bonding. While albeit for only a limited data set, this suggests that $j \propto$ reaction rate $\propto e^{-\Delta E^{\ddagger}/RT}$, where $\Delta E^{\ddagger}$ is an "activation energy", which can be expected to be influenced by the $2\pi^*$ E_f-LDOS. Note also that under our actual current generating conditions, the concentrations of CO on Pt/Ru will be very small, so that the CO on Pt/Ru diffusion measurements described above do not permit a direct determination of any diffusional contribution to $\Delta E^{\ddagger}$, although they do give clear evidence for the lack of rapid diffusion between domains.

Conclusions

The results we have described above are of interest for a number of reasons. First, we have obtained ^{13}C/EC NMR spectra of Pt/Ru catalysts of interest in DMFC applications. The results give evidence for two ^{13}CO domains: CO on both Pt and Pt/Ru sites. Second, we have obtained static potentiostatic currents and CV results for these catalysts. The CV results also give evidence for two domains, and there is a 1:1 relationship between the NMR and CV peak areas, thereby correlating the electrochemical and NMR results. Third, we have found that COs on Pt/Ru domains have NMR resonances highly shifted from those of the Pt/CO domains, have small Knight shifts, and weak Korringa relaxation. These results imply a major decrease in both metal and ligand E_f-LDOS. Fourth, our results show that COs on the Pt/Ru domains exhibit thermally activated diffusive motion, from which the activation energies for diffusion can be estimated. Ruthenium decreases the activation barrier for diffusion by reducing back-donation. Fifth, our results indicate there is an excellent correlation ($R = 0.994$, $p = 0.006$) between the $2\pi^*$ E_f-LDOS values for CO on Pt and the steady-state currents seen in the electrochemical measurements. The linear relation between ln j and E_f(LDOS) suggests that as back-bonding to CO on Pt decreases (due to long-range electronic effects of Ru doping), the current increases. Sixth, the NMR results show there is essentially no exchange between the two CO species, consistent with the CV data.

When taken together, these results are of general interest since they represent the first correlations between classical electrochemical techniques (CV, static current generation) and electrochemical NMR results (peak intensities for assignments, E_f-LDOS measurements for bonding, E_{diff} for diffusional barriers) which in the future may lead to even more detailed insights into the mechanisms of action of promoters in fuel cell applications, in particular, and heterogeneous catalysis, in general.

Acknowledgment. The authors thank Professor R. Masel for very stimulating discussions. This work was supported by the United States National Science Foundation (grant CTS 97-26419), by an equipment grant from the United States Defense Advanced Research Projects Agency (grant DAAH 04-95-1-0581), and by the U.S. Department of Energy under Award No. DEFG02-96ER45439.

JA011729Q

(20) McBreen, J.; Mukerjee, S. In *Interfacial Electrochemistry: Theory, Experiment, and Applications*; Wieckowski, A., Ed.; Marcel Dekker: New York, 1999; pp 895−914.
(21) Rice, C.; Tong, Y. Y.; Oldfield, E.; Wieckowski, A.; Hahn, F.; Gloaguen, F.; Leger, J.-M.; Lamy, C. *J. Phys. Chem. B* **2000**, *104*, 5803−5807.